

Enzyme structural plasticity and the emergence of broad-spectrum antibiotic resistance

Frédérique Maurice¹, Isabelle Broutin¹, Isabelle Podglajen², Philippe Benas¹, Ekkehard Collatz²
& Frédéric Dardel^{1*}

¹Cristallographie and RMN Biologiques, Université Paris Descartes, CNRS, Paris, France, and ²Laboratoire de Recherche Moléculaire sur les Antibiotiques, Université Paris 6, Paris, France

The emergence of multi-resistant pathogenic bacteria is a worldwide health issue. Recently, clinical variants of a single antibiotic-modifying acetyltransferase, AAC(6′)-Ib—a variant of aminoglycoside 6′-N-acetyltransferase—have been identified that confer extended resistance to most aminoglycosides and, more surprisingly, to structurally unrelated fluoroquinolones. The corresponding gene is carried by mobile genetic elements and is present in most multi-resistant pathogenic strains, hence making it a serious threat to current therapies. Here, we report the crystal structures of both narrow- and broad-spectrum resistance variants of this enzyme, which reveal the structural basis for the emergence of extended resistance. The active site shows an important plasticity and has adapted to new substrates by a large-scale gaping process. We have also obtained co-crystals with both substrates, and with a simple transition state analogue, which provides new clues for the design of inhibitors of this resistance mechanism.

Keywords: acetyltransferase; aminoglycoside; antibiotic resistance; ciprofloxacin; crystallography

EMBO reports (2008) 9, 344–349. doi:10.1038/embor.2008.9

INTRODUCTION

One of the main mechanisms of antibiotic resistance is the enzymatic modification of the active compound, which prevents its binding to the cellular target. Aminoglycosides and fluoroquinolones are potent, broad-spectrum antibiotics of clinical importance. Until recently, they avoided this resistance mechanism to varying degrees, which preserved them as crucial drugs for treating life-threatening infections caused by resistant bacteria. Although no enzymatic modification of the synthetic fluoroquinolones

has been observed, the known aminoglycoside-modifying enzymes, with their somewhat limited substrate specificities, could not simultaneously inactivate all clinically used compounds. One of the most common mechanisms is N-acetylation at the 6′ position (Vakulenko & Mobashery, 2003; Fig 1A), catalysed by the aminoglycoside 6′-N-acetyltransferase (AAC(6′)). Two functional classes of this enzyme have been described: AAC(6′)-I, which confers resistance to amikacin but not to gentamicin, and AAC(6′)-II, with the reciprocal selectivity; both classes also acetylate kanamycin, tobramycin, neomycin, netilmicin and sisomicin. Now, isoforms of the AAC(6′)-Ib subclass have evolved in clinical isolates with the ability to modify amikacin and gentamicin or some fluoroquinolones.

This has a strong clinical relevance as AAC(6′)-Ib is the most prevalent aminoglycoside-modifying enzyme, present in more than 70% of AAC(6′)-producing Gram-negative isolates (Vakulenko & Mobashery, 2003). Its spread might have been favoured by integration of its gene into natural expression vectors such as integrons (Fluit & Schmitz, 2004). Among the recent variants of this enzyme with altered specificity are AAC(6′)-Ib₁₁, which confers simultaneous resistance to gentamicin and amikacin (Casin *et al*, 2003), and AAC(6′)-Ib-cr, which has a unique extension of its substrate specificity from aminoglycosides to structurally unrelated fluoroquinolones (Robicsek *et al*, 2006a). Both variants differ from the initially identified AAC(6′)-Ib (Tran Van Nhieu & Collatz, 1987) by two amino-acid substitutions each and by functionally irrelevant amino-terminal differences (Robicsek *et al*, 2006b; supplementary Fig 1 online).

Two structures of AAC(6′)-I have been reported: AAC(6′)-Ii and AAC(6′)-Iy (Wybenga-Groot *et al*, 1999; Vetting *et al*, 2004). These two enzymes are chromosomally encoded and hence confined to a single bacterial species. They confer a low level of resistance and their primary function as aminoglycoside resistance enzymes has been questioned (Magnet *et al*, 2001). Accordingly, they have moderate catalytic efficiencies and/or affinities for aminoglycosides, approximately one to two orders of magnitude lower than those of AAC(6′)-Ib (Wright & Ladak, 1997; Magnet *et al*, 2001; Kim *et al*, 2007). Their sequences are also divergent from those of the predominant AAC(6′)-Ib (identity level <20%;

¹Cristallographie and RMN Biologiques, Université Paris Descartes, CNRS, 4 Avenue de l'Observatoire, 75006 Paris, France

²Laboratoire de Recherche Moléculaire sur les Antibiotiques, Université Paris 6, 15 Rue de l'École de Médecine, 75006 Paris, France

*Corresponding author. Tel: +33 1 53 73 95 12; Fax: +33 1 53 73 99 25; E-mail: frederic.dardel@univ-paris5.fr

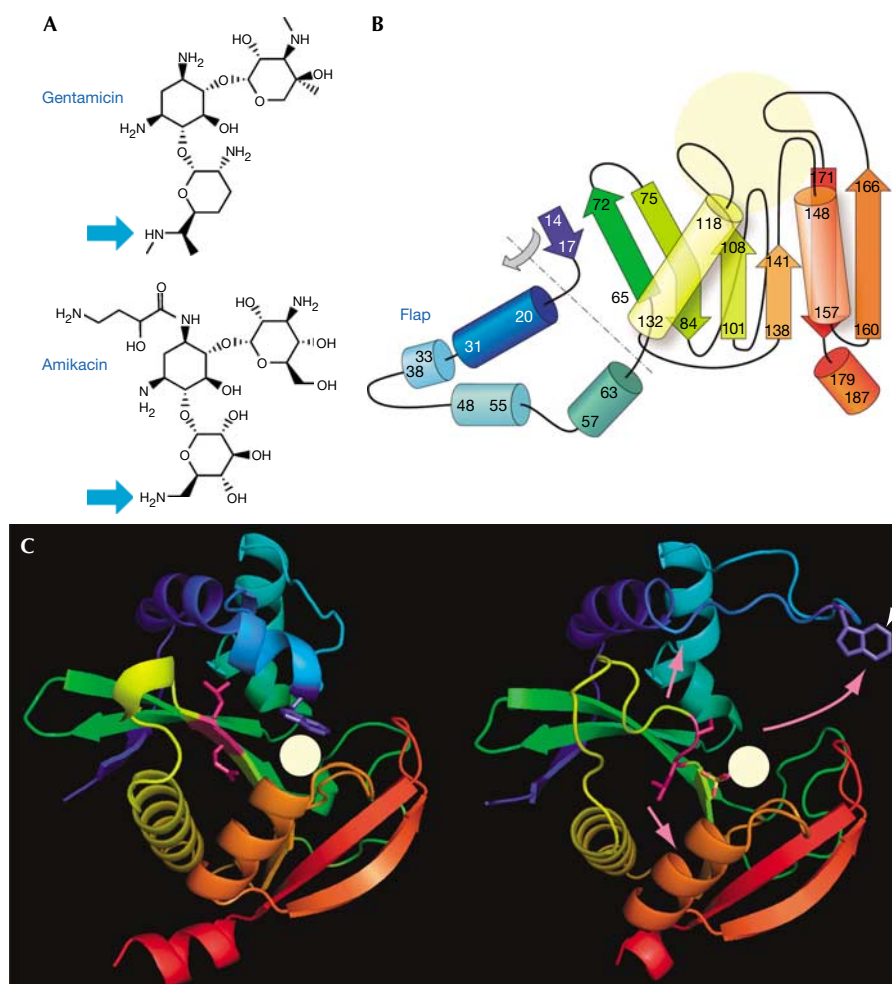


Fig 1 | Structure of AAC(6')-Ib and the structural switch associated with broad-spectrum inducing substitutions. (A) Structure of gentamicin and amikacin. The amino groups that are acetylated are indicated by arrows. (B) Topology of AAC(6')-Ib. Residue numbers are indicated. The yellow disk indicates the location of the aminoglycoside-binding pocket. The top of this pocket is closed by an α -helical flap, which folds back along the dashed axis, above the central β -sheet. (C) Structure of AAC(6')-Ib (left) and its broad-spectrum variant AAC(6')-Ib₁₁ (right). Substituted residues are shown in purple (arrowhead). Pink arrows indicate movements of the flap and Trp38. The same colour coding is used for (B) and (C). AAC(6'), aminoglycoside 6'-N-acetyltransferase.

supplementary Fig 1 online); therefore, they cannot be used to provide structural insights into the broadening of AAC(6')-Ib specificity and its current clinical consequences.

Here, we report the structure of narrow- and broad-spectrum variants of AAC(6')-Ib, free and as a complex. Interaction with the antibiotic substrate is different from that of AAC(6')-Iy and allows both tighter binding and broader recognition of second-generation aminoglycosides such as amikacin. Furthermore, we show that the mutations that are responsible for spectrum broadening induce a large structural change in the active site, which allows for the accommodation of an extended set of substrates.

RESULTS AND DISCUSSION

We have solved the crystal structures of both AAC(6')-Ib and AAC(6')-Ib₁₁. The narrow-spectrum variant Ib was crystallized in complex with coenzyme A (CoA; structure solved to 1.8 Å resolution), or coenzyme A and kanamycin (2.4 Å resolution).

Crystals of the broad-spectrum variant Ib₁₁ were obtained in the absence of substrate (2.1 Å resolution). Interestingly, each variant failed to crystallize under the conditions used for the other variant. Both variants share the same fold (Fig 1B), which belongs to the GCN5-related N-acetyltransferase superfamily (Vetting *et al*, 2005), which also encompasses other classes of AAC. Accordingly, the acetyl-CoA binding site is structurally similar to that of other enzymes in this family. Even if the cofactor was not co-crystallized with AAC(6')-Ib₁₁, the corresponding binding pocket is similar to that of AAC(6')-Ib (supplementary Fig 2 online). There are, however, important differences at the level of the antibiotic-binding site, which will be discussed below.

The two previously reported AAC(6') structures are dimers and their aminoglycoside-binding crevice is shared between the two protomers (Wybenga-Groot *et al*, 1999; Vetting *et al*, 2004; supplementary Fig 3 online). Conversely, AAC(6')-Ib is essentially monomeric: gel filtration experiments confirmed that AAC(6')-Ib

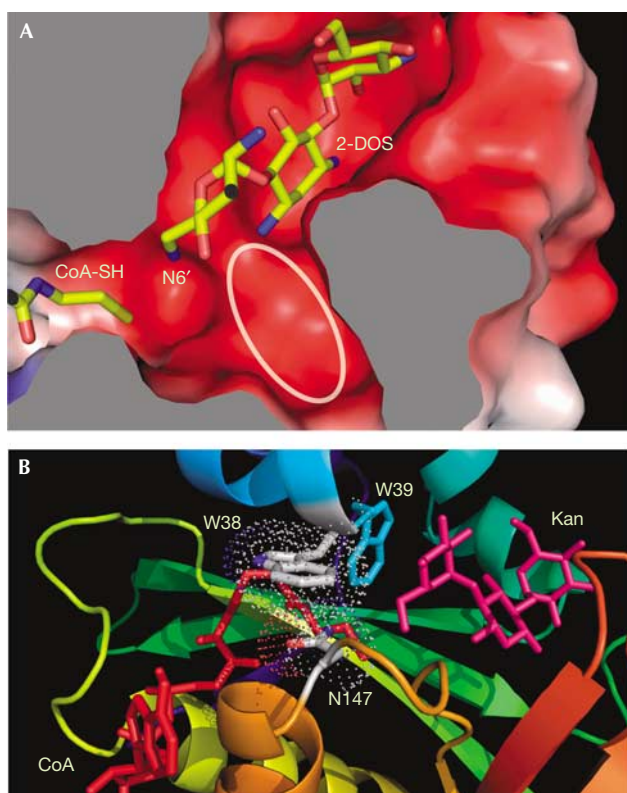


Fig 2 | Recognition of ligands. (A) Structure of AAC(6')-Ib in complex with kanamycin (Kan). The solvent-accessible surface is shown, coloured as a function of the electrostatic surface potential. The oval contour highlights the crevice that could accommodate N3 substituents of 2-deoxystreptamine (2-DOS) such as that present in amikacin. (B) Locking of the 'flap' around coenzyme A (CoA). Asn (N) 146 is hydrogen bonded to the pantetheine arm and provides a stacking platform for the side chain of Trp (W) 38 in the flap. This contributes to position W39, which is part of the antibiotic-binding pocket. AAC(6'), aminoglycoside 6'-N-acetyltransferase.

and AAC(6')-Ib-cr are monomers in solution, whereas AAC(6')-Ib₁₁ shows a monomer/dimer equilibrium (data not shown). Accordingly, the active site is contained within a single protomer, with the aminoglycoside-binding site being constituted by connecting loops (Fig 1B), a topology that differs from the previously reported structures. These loops form a closed pocket, in which the aminoglycoside fits snugly (Fig 2A).

There is also a long α -helical flap that forms a lid over the antibiotic pocket, with a loop that is in contact with the aminoglycoside rings (Fig 1B). This extended flap is specific to ACC(6')-Ib (supplementary Figs 1,3 online) and is held in place by a stacking interaction between the side chains of Trp 38 (in the flap) and Asn 147 (in the core; Fig 2B), creating a tunnel surrounding the end of the pantetheine arm of coenzyme A. This could explain the specific enzymatic behaviour of AAC(6')-Ib, which shows an ordered kinetic mechanism in which acetyl-CoA is the first substrate to bind (Kim *et al*, 2007). Locking of the flap around acetyl-CoA could therefore position crucial residues involved in antibiotic recognition, such as Trp 39, which stacks onto

the aminoglycoside ring I. Hence, prior binding of acetyl-CoA could facilitate subsequent recognition of the antibiotic.

AAC(6')-Ib has evolved the ability to acetylate semisynthetic aminoglycosides that carry a bulky N-substituent on the central ring, such as amikacin (Fig 1A). Indeed, a cavity exists on the surface of the active site that could accommodate such a chain (Fig 2A). This binding pocket is absent in the active site of other, less-efficient variants of AAC(6').

Mutations that confer a broadened spectrum to AAC(6')-Ib₁₁, Q106L and L107S (purple in Fig 1C), are not located in the immediate vicinity of the aminoglycoside site, but along the narrow groove that binds to the pantetheine arm of acetyl-CoA. In AAC(6')-Ib₁₁, the double substitution induces a large structural change, caused by a disruption of the central β -strand (Fig 1C; supplementary Fig 4 online). As a consequence, packing of the helices above and below the β -sheet is perturbed, causing a large-scale 'gaping' of the active site, with Trp 38 moving by as much as 15 Å. Several lines of evidence indicate that this structural change is genuine and not a consequence of crystal packing. It is a direct structural effect: in the wild-type structure, the side chain of Trp 39, in the flap, interdigitates between residues 105 and 107, an interaction that is obstructed by the double mutation at this site (supplementary Fig 4 online). This structural change involving Trp 38 and Trp 39 also induces a redshift of the intrinsic fluorescence of the mutant protein in solution, suggesting that they are indeed more exposed to the solvent in the latter structure (supplementary Table 1 online). It is thus likely that the flap will be flexible in the AAC(6')-Ib₁₁ mutant with several possible conformations. These structural changes result in a marked increase in the accessible volume of the active site, which could then possibly accommodate bulkier substrates with substituted amino groups. In addition, the carboxylate group of Asp 105, next to the double mutation, could also contribute directly to render the secondary N6' amine of gentamicin more acidic and therefore more reactive to acetylation (supplementary Fig 5 online). This might explain the dual specificity of this variant for gentamicin and amikacin.

AAC(6')-Ib₁₁, which was crystallized in the absence of substrate, co-crystallized with one HEPES buffer molecule bound within the active site (Fig 3B). Remarkably, the sulphonate group of HEPES lies over the position of the sulphur atom of coenzyme A and the nitrogen atom of its piperazine ring sits at the site of the acetyltable nitrogen of kanamycin. By using solution nuclear magnetic resonance (NMR), we observed direct saturation transfer from the protons of the enzyme to those of HEPES, confirming that HEPES is able to bind to AAC(6') not only in crystals, but also in solution (supplementary Fig 6 online). Hence, HEPES seems to be a minimal transition state analogue of the acetylation reaction (Fig 3A) and could thus be used as a central scaffold for building effective inhibitors of AAC(6') enzymes.

Interestingly, one of the fluoroquinolones that AAC(6')-Ib-cr has evolved to recognize—ciprofloxacin—also contains a piperazine moiety (Fig 3A), which is N-acetylated by the enzyme (Robicsek *et al*, 2006a). The two substitutions that confer the new specificity to AAC(6')-Ib-cr—W92R and D169Y—are located in two exposed loops, which form the posterior side of the antibiotic-binding pocket (Fig 1B). Therefore, it seems straightforward to model the structure of AAC(6')-Ib-cr based on that of AAC(6')-Ib. The interaction with ciprofloxacin was also investigated, using the structural similarity with HEPES to anchor the piperazine ring of

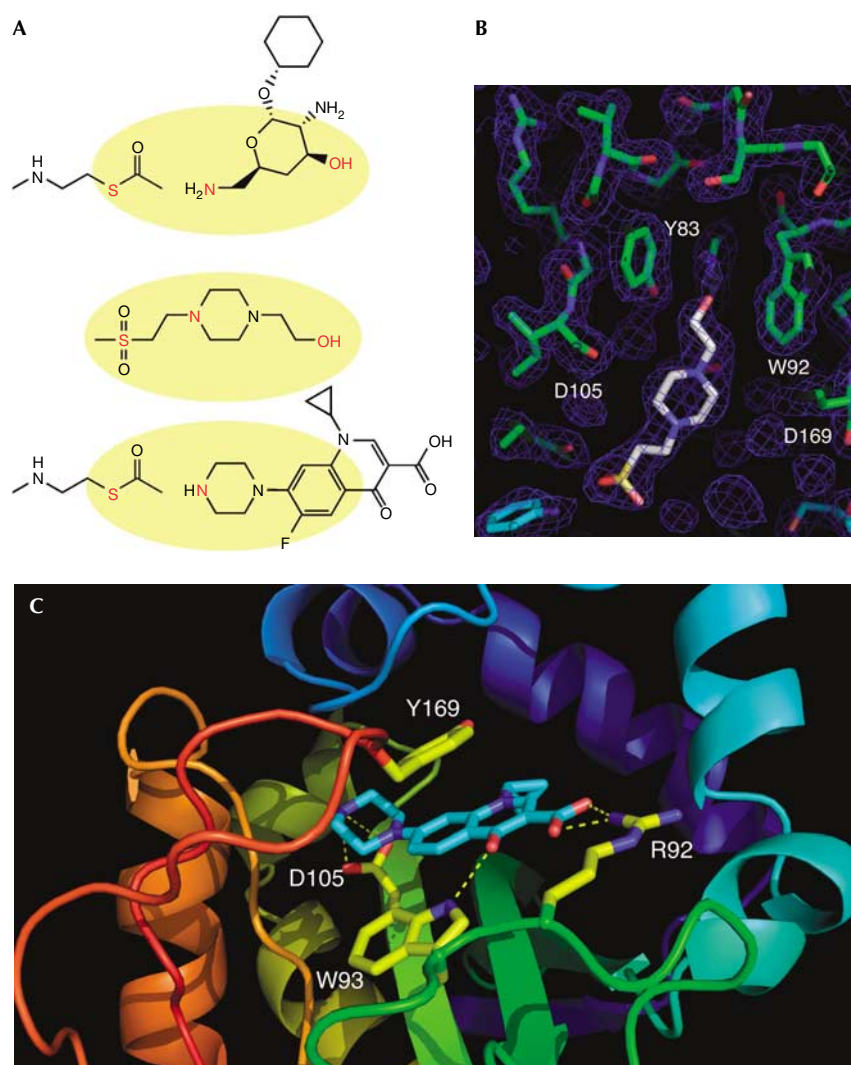


Fig 3 | Interaction of AAC(6′)-Ib with ligands. (A) Comparison of ligand geometries. Top, acetyl-coenzyme A (CoA) and aminoglycoside; middle, HEPES; bottom, acetyl-CoA and ciprofloxacin. (B) $2F_o - F_c$ electron density maps of HEPES bound in the active site of AAC(6′)-Ib₁₁ contoured at 2σ . (C) Refined model of ciprofloxacin bound to AAC(6′)-Ib-cr, showing interactions with the two mutated residues, R92 and Y169 (same colour coding as in Fig 1). AAC(6′), aminoglycoside 6′-N-acetyltransferase. D, Asp; R, Arg; W, Trp; Y, Tyr.

the fluoroquinolones in the enzyme. The result of this modelling (Fig 3C) shows the side chains of the two substituted residues being in a position to form specific stabilizing interactions with ciprofloxacin: Tyr 169 can stack on the quinolone heterocycle, whereas the guanidinium group of Arg 92 can hydrogen bond to the keto or carboxy groups of the antibiotic.

In addition to the ‘gaping’ ability of the active site, the specific scaffold of AAC(6′)-Ib, in which recognition of the acetyltable substrate is mediated by the side chains of the exposed loops (as opposed to other AAC(6′) enzymes), could provide the structural plasticity required for adaptation to new antibiotics. This could explain, in part, why this isoform has been selected under the pressure of antibiotic usage and is now widely distributed among pathogens. Conversely, such a broad distribution makes AAC(6′)-Ib an attractive target for countering drug resistance. The reported structures could help in guiding the

design of new aminoglycosides that avoid resistance. In addition, the observation that an original scaffold—piperazine ethane sulphonate—can mimic the transition state, could be an interesting lead for designing new inhibitors.

METHODS

Plasmid construction and protein expression. AAC(6′)-b₁₁ was originally identified in *Salmonella enterica* (Casin *et al*, 2003). Its sequence was PCR amplified and cloned in pET101 (Invitrogen, Carlsbad, CA, USA) and expressed in *Escherichia coli* (Maurice *et al*, 2006). This protein showed a significant propensity to aggregate and was expressed in inclusion bodies at growth temperatures above 20 °C. We used a phenotypic screen to select for increased solubility. Transformed *E. coli* cells were streaked on LB plates containing kanamycin (50 µg/ml) and incubated at 37 °C. Cells expressing soluble AAC(6′)-Ib were able to grow

normally as they could acetylate the antibiotic, whereas those expressing insoluble forms were selected against. After DNA sequencing, one such resistant variant was found to carry a single nucleotide deletion in the stop codon. This results in a carboxy-terminal extension of the protein by a hydrophilic tail of seven amino acids, EGRAQFE (supplementary Fig 1 online). This 'tagged' variant proved to be stable and soluble. This was subjected to further studies, as it is otherwise identical to the original AAC(6′)-Ib₁₁ and shows a similar antibiotic selectivity. Purification of this protein was achieved as described previously (Maurice *et al*, 2006). Expression vectors for wild-type AAC(6′)-Ib and variant AAC(6′)-Ib-cr were derived by site-directed mutagenesis of the AAC(6′)-Ib₁₁ vector (QuikChange, Stratagene, La Jolla, CA, USA) and the corresponding proteins also contained the solubility tag. The function of these AAC(6′)-Ib variants was monitored by *in vivo* functional resistance assays (supplementary Table 2 online).

Protein crystallization. Crystals of AAC(6′)-Ib were grown at 18 °C by using the hanging-drop method from a solution containing 1.5 M K₂HPO₄, 0.06 M NaH₂PO₄ and 0.1 M guanidine-HCl, and were reproduced by streak seeding. Crystals were stabilized in 15% glycerol, 1.6 M K₂HPO₄ and 0.07 M NaH₂PO₄ before vitrification in liquid N₂. Crystals belong to space group P₄₃2₁2 with unit cell constants of $a = b = 57.62$ Å and $c = 146.67$ Å.

Crystals of AAC(6′)-Ib₁₁ and Se-Met-AAC(6′)-Ib₁₁ were grown at 18 °C using the hanging-drop method by mixing equal volumes of protein (15 mg/ml) and reservoir solution (100 mM HEPES pH 7.5, 1.5 M Li₂SO₄ and 3% isopropanol). Crystals belong to space group C222₁ with unit cell constants of $a = 71.62$ Å, $b = 85.37$ Å and $c = 150.41$ Å.

Structural determination and refinement. A multi-wavelength anomalous diffraction data set was collected on a Se-Met AAC(6′)-Ib₁₁ crystal to 2.8 Å resolution on the BM30A beam line (ESRF, Grenoble, France). Data sets were collected at $\lambda = 0.9794$ Å (inflexion), $\lambda = 0.9792$ Å (peak) and $\lambda = 0.9278$ Å (remote). They were integrated and scaled with X-ray detection software (Kabsch, 1993). Model building was performed with Sharp and O (Jones *et al*, 1991). A 2.1 Å resolution native data set of AAC(6′)-Ib₁₁ was also collected on ID14 (ESRF, Grenoble, France) and the refinement was performed in CNS (Brunger *et al*, 1998; see supplementary Table 3 online for crystallographic parameters).

The structure of AAC(6′)-Ib was solved with Phaser (Read, 2001) using AAC(6′)-Ib₁₁ as a molecular replacement model. The model was completed by using iterative cycles of model building and refinement in REFMAC (Winn *et al*, 2001). Although not added in the crystallization solution, electron density owing to bound coenzyme A was observed, a situation previously reported for AAC(6′)-Iy (Vetting *et al*, 2004). The structure of the complex with kanamycin was obtained by diffusing the antibiotic into the crystals (1:1 ratio with the protein) and solving the structure similarly. $2F_o - F_c$ density maps of coenzyme A and kanamycin are shown in supplementary Fig 7 online.

Completeness of the models was 173 out of 196 residues for both the AAC(6′)-Ib and AAC(6′)-Ib₁₁ structures. Density was missing for residues 1–10 and 184–196 in AAC(6′)-Ib₁₁, and for residues 1–11, 41–43 and 188–196 in AAC(6′)-Ib. The missing N- and C-terminal extensions are not part of the enzyme core. The C-terminal extension corresponds to the solubility tag, whereas the N-terminal extension originates from gene fusion (Casin *et al*, 1998).

AAC(6′)-Ib₁₁ crystals contain two monomers per asymmetrical unit, whereas the wild-type enzyme contains only one and is a true monomer in solution (data not shown). The former observation could be related to the fact that AAC(6′)-Ib₁₁ variant seems to be partly dimeric in gel filtration experiments (data not shown). The protein–protein contact seen in the crystal structure of this protein differs from that observed in the structure of other AAC(6′) variants.

Coordinates have been deposited with the Protein Data Bank, entries 2PRB, 2QIR and 2PR8.

Saturation transfer difference. NMR set-up and saturation transfer difference experiments (Mayer & Meyer, 2001) using AAC(6′)-Ib₁₁ were performed as described previously (Tisne & Dardel, 2002; Maurice *et al*, 2006).

Modelling the interaction with ciprofloxacin. Starting from the structure of wild-type AAC(6′)-Ib, the two mutations, W92R and D169Y (supplementary Fig 1 online), were introduced manually using Pymol (DeLano Scientific, Palo Alto, CA, USA). The corresponding structure was energy minimized by using X-PLOR-NIH (Schwieters *et al*, 2003). Ciprofloxacin structure was generated using PRODRG (Schuttelkopf & van Aalten, 2004). Six different rotamers of ciprofloxacin were generated, by rotation about the piperazine–quinolone bond. They were then placed into the active site of AAC(6′)-Ib-cr by superimposing their piperazine ring onto that of HEPES in the structure of AAC(6′)-Ib₁₁ and ignoring steric clashes. These six complexes were refined independently. C α atoms of residues outside the active site—residues 12–38, 44–87, 95–163 and 174–187—were restrained by a harmonic potential, as well as the acetylable nitrogen of ciprofloxacin, to maintain the active site geometry. The complex was energy minimized and submitted to a restrained simulated annealing refinement. It consisted of 2 ps of dynamics at 1,000 K followed by cooling to 100 K over 10 ps during which the harmonic restraints on the C α atoms were gradually turned off. The resulting complexes were finally energy minimized.

Of the six resulting structures, two had poor energy scores and were discarded. The remaining four structures were very similar, with both rings of ciprofloxacin in comparable orientations. In some structures, the mutated residues—Arg 92 and Tyr 169—had come in contact with the ligand, indicating that they contributed directly to binding. To model these interactions, we submitted the four structures to an additional short restrained molecular dynamics refinement (5 ps at 100 K followed by minimization). We added distance restraints, forcing the guanidinium of Arg 92 and the ring of Tyr 169 to contact ciprofloxacin. This resulted in structures in which Arg 92 contacted the oxo or carboxy oxygen of ciprofloxacin, whereas Tyr 169 stacked on top of the quinolone. All four structures were similar and had good stereochemistry. The best structure is shown in Fig 3C.

Supplementary information is available at *EMBO reports* online (<http://www.emboreports.org>).

ACKNOWLEDGEMENTS

We acknowledge Dr C. Mayer and Dr S. Biarrotte-Sorin for initial advice on structure determination. F.M. is supported by a scholarship from the French Ministry of research and higher education.

CONFLICT OF INTEREST

The authors declare that they have no conflict of interest.

REFERENCES

- Brunger AT *et al* (1998) Crystallography & NMR system: a new software suite for macromolecular structure determination. *Acta Crystallogr D* **54**: 905–921
- Casin I, Bordon F, Bertin P, Coutrot A, Podglajen I, Brasseur R, Collatz E (1998) Aminoglycoside 6'-N-acetyltransferase variants of the Ib type with altered substrate profile in clinical isolates of *Enterobacter cloacae* and *Citrobacter freundii*. *Antimicrob Agents Chemother* **42**: 209–215
- Casin I, Hanau-Bercot B, Podglajen I, Vahaboglu H, Collatz E (2003) *Salmonella enterica* serovar Typhimurium bla(PER-1)-carrying plasmid pST11 encodes an extended-spectrum aminoglycoside 6'-N-acetyltransferase of type Ib. *Antimicrob Agents Chemother* **47**: 697–703
- Fluit AC, Schmitz FJ (2004) Resistance integrons and super-integrons. *Clin Microbiol Infect* **10**: 272–288
- Jones TA, Zou JY, Cowan SW, Kjeldgaard M (1991) Improved methods for building protein models in electron density maps and the location of errors in these models. *Acta Crystallogr A* **47**: 110–119
- Kabsch W (1993) Automatic processing of rotation diffraction data from crystals of initially unknown symmetry and cell constants. *J Appl Crystallogr* **26**: 795–800
- Kim C, Villegas-Estrada A, Hesek D, Mobashery S (2007) Mechanistic characterization of the bifunctional aminoglycoside-modifying enzyme AAC(3)-Ib/AAC(6')-Ib' from *Pseudomonas aeruginosa*. *Biochemistry* **46**: 5270–5282
- Magnet S, Lambert T, Courvalin P, Blanchard JS (2001) Kinetic and mutagenic characterization of the chromosomally encoded *Salmonella enterica* AAC(6')-Iy aminoglycoside N-acetyltransferase. *Biochemistry* **40**: 3700–3709
- Maurice F, Bégis B, Micouin L, Dardel F (2006) NMR identification of ligands of aminoglycoside resistance enzymes. *C R Chimie* **9**: 413–419
- Mayer M, Meyer B (2001) Group epitope mapping by saturation transfer difference NMR to identify segments of a ligand in direct contact with a protein receptor. *J Am Chem Soc* **123**: 6108–6117
- Read RJ (2001) Pushing the boundaries of molecular replacement with maximum likelihood. *Acta Crystallogr D* **57**: 1373–1382
- Robicsek A, Strahilevitz J, Jacoby GA, Macielag M, Abbanat D, Park CH, Bush K, Hooper DC (2006a) Fluoroquinolone-modifying enzyme: a new adaptation of a common aminoglycoside acetyltransferase. *Nat Med* **12**: 83–88
- Robicsek A, Jacoby GA, Hooper DC (2006b) The worldwide emergence of plasmid-mediated quinolone resistance. *Lancet Infect Dis* **6**: 629–640
- Schuttelkopf AW, van Aalten DM (2004) PRODRG: a tool for high-throughput crystallography of protein–ligand complexes. *Acta Crystallogr D* **60**: 1355–1363
- Schwieters CD, Kuszewski JJ, Tjandra N, Clore GM (2003) The Xplor-NIH NMR molecular structure determination package. *J Magn Reson* **160**: 65–73
- Tisne C, Dardel F (2002) Optimisation of a peptide library for screening specific RNA ligands by flow-injection NMR. *Comb Chem High Throughput Screen* **5**: 523–529
- Tran Van Nhieu G, Collatz E (1987) Primary structure of an aminoglycoside 6'-N-acetyltransferase AAC(6')-4, fused *in vivo* with the signal peptide of the Tn3-encoded β -lactamase. *J Bacteriol* **169**: 5708–5714
- Vakulenko SB, Mobashery S (2003) Versatility of aminoglycosides and prospects for their future. *Clin Microbiol Rev* **16**: 430–450
- Vetting MW, Magnet S, Nieves E, Roderick SL, Blanchard JS (2004) A bacterial acetyltransferase capable of regioselective N-acetylation of antibiotics and histones. *Chem Biol* **11**: 565–573
- Vetting MW, LP SdC, Yu M, Hegde SS, Magnet S, Roderick SL, Blanchard JS (2005) Structure and functions of the GNAT superfamily of acetyltransferases. *Arch Biochem Biophys* **433**: 212–226
- Winn MD, Isupov MN, Murshudov GN (2001) Use of TLS parameters to model anisotropic displacements in macromolecular refinement. *Acta Crystallogr D* **57**: 122–133
- Wright GD, Ladak P (1997) Overexpression and characterization of the chromosomal aminoglycoside 6'-N-acetyltransferase from *Enterococcus faecium*. *Antimicrob Agents Chemother* **41**: 956–960
- Wybenga-Groot LE, Draker K, Wright GD, Berghuis AM (1999) Crystal structure of an aminoglycoside 6'-N-acetyltransferase: defining the GCN5-related N-acetyltransferase superfamily fold. *Structure* **7**: 497–507